Experiments in Fluids 3, 343–348 (1985)

Experiments in Fluids

Effect of symmetry and asymmetry of turbulent structures on the interaction region of a plane jet

A. J. Chambers, R. A. Antonia, and **L. W. B. Browne**

Department of Mechanical Engineering, University of Newcastle, N.S.W., 2308, Australia

Abstract. Mean and rms velocity and temperature measurements are made in the near field of a plane jet for two different sets of conditions at the beginning of the interaction region. In the first, the jet has a nearly top-hat velocity profile and laminar boundary layers at the nozzle exit. Schlieren photography and spectral coherence measurements show that the mixing layer structures are strongly organised and symmetric about the centreline. In the second, the jet issues from a two-dimensional duct with a nearly fully developed velocity profile so that, upstream of the interaction region, turbulent structures should be three-dimensional and asymmetric about the jet centreline. The resulting weak interaction obtained in this case contrasts with the strong interaction measured in the first case.

1 Introduction

In a recent paper (Browne et al. 1984) several turbulence quantities were measured in the interaction region of a plane jet, beginning downstream of the potential core and extending to the nearly self-preserving far field region. A strong interaction was found between opposite mixing layers at the end of the potential core. This contrasted with the relatively weak interaction observed by Weir et al. (1981) who found that a "time-sharing" superposition calculation, optimised for a single mixing layer, produced fairly satisfactory results in the interaction region. The initial boundary layers were laminar in both experiments but Browne et al. suggested that the strong interaction in their experiment was a result of the symmetric nature of the mixing layer structures. An asymmetric arrangement may have existed in Weir et al.'s experiment, possibly as a result of a coherent flapping oscillation of the whole jet (Weir & Bradshaw 1975).

It seemed of interest to investigate the effect on the interaction region of two different types of conditions prior to the merging of the mixing layer. The two specific conditions that we initially intended to study were the symmetric and asymmetric mixing layer structures, both associated with laminar shear layers at the nozzle lips. The first was naturally achieved in the present flow, but attempts[1] to achieve asymmetry, as reported for example by Rockwell and Niccolls (1972) and more recently by Hussain (1983), were unsuccessful. While the causes for either symmetry or asymmetry are not understood, there is evidence (Oseberg & Kline 1971; Hussain 1983) that the symmetric mode prevails (at least for an initial top-hat profile with laminar boundary layers) perhaps because the pressure field disturbance that arises from the instability of either shear layer triggers a symmetric instability in the opposite shear layer. A plausible contender for the asymmetric condition seemed to be a jet emerging from a two-dimensional turbulent duct flow. Dean and Bradshaw (1976) indicated that turbulent structures or large eddies on opposite sides of the duct centreline simply time-share across the centreline; a superposition analysis, optimised on a single boundary layer, yielded good results.

This paper primarily documents the two different conditions at the start of the interaction region and the corresponding centreline distributions of mean and rms velocity and temperature in the interaction region. These resulting distributions indicate significantly different types of interaction between the two conditions.

2 Experimental arrangement and initial conditions

The basic plane jet facility, described in more detail in Antonia et al. (1983a), consists of a variable speed centrifugal squirrel cage blower supplying air to a two-dimensional 20:1 contraction. For configuration A (Fig. 1a) the jet exists normally to an end plate (approximately 255×280 mm) from a slit, of width $d = 12.7$ mm and span 250 mm, centrally located in this plate.

1 These included tripping one of the shear layers but not, for example, external acoustic excitation. A laminar channel flow was tried but, unlike the observation of Hussain (1983), an alternate rolling up of vortices in opposite shear layers was not observed

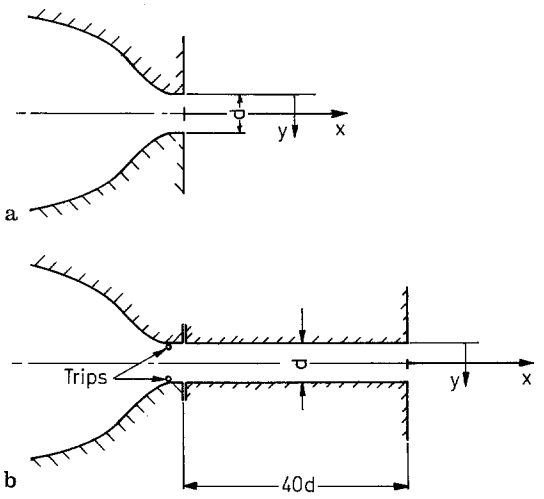

Fig. 1 a and b. Sketch of the plane jet exit configurations and system of co-ordinates. **a:** A; **b:** B

For configuration B, the jet exits from a rectangular duct (width $d = 12.7$ mm, span = 250 mm and length $\simeq 510$ mm) fastened to the exit of the two-dimensional contraction of the jet facility. Two 0.5 mm diameter trips were stretched across the full span of the slit, immediately upstream of the entrance to the duct. Comte-Bellot (1963) found that a useful indication of fully-developed turbulent flow is provided by the streamwise variation of the skewness and flatness factors of the velocity fluctuation u. For a fully developed duct flow, these parameters should be independent of x. The present investigation was made with R_d ($= \bar{U}_j d/\nu$, where $\bar{U}_j$ is the maximum jet exit velocity and ν is the kinematic viscosity of air) $\simeq 7600$. The duct measurements of Shah et al. (1984) indicate that, for this Reynolds number, the skewness and flatness factors of u become approximately constant at $x/d = 40$. Thus the length of the add-on duct was made 40 d.

For both configurations, the jet was heated with 1 kW electrical coil elements located immediately downstream of the blower. The nominal mean jet exit temperature $\bar{T}_j$ was 22 °C above ambient. The temperature was used as a passive marker of the flow and to provide the density gradients needed for the schlieren photography.

Measurements of velocity and temperature fields were made using single hot and cold wires. The hot and cold wires (Pt-10% Rh Wollaston) were 0.6 mm in length and had diameters of 5 μm and 0.63 μm respectively. The hot wire was operated with a constant temperature anemometer (DISA 55M10) at an overheat of 0.8. The cold wire was operated at constant current (= 0.1 mA) using in-house anemometers. Signals from the anemometers were recorded on an FM tape recorder (HP3968A) after appropriate signal conditioning. These signals were later digitised at 2 kHz and digital recorders of approximately 2 min. duration were processed on a PDP 11/34 computer. The digital hot wire voltages were corrected for temperature contamination before converting to fluctuating velocities.

The hot and cold wires were calibrated at the jet exit. The exit velocity of the jet was measured using a pitot-static tube connected to a Furness micromanometer with a resolution of 0.01 mm H_2O. For the temperature calibration, a 10 Ω platinum resistance thermometer was operated with a Leeds and Northrup 8078 bridge and gave a mean temperature sensitivity of ± 0.01 °C. A data logger consisting of a data acquisition system (HP3497A) and a desk top computer (HP85) were used to process the calibration information and monitor the performance of the two wires during an experiment.

The mean exit velocity profile (Fig. 2) for A is in good agreement with the Blasius distribution. The profile was

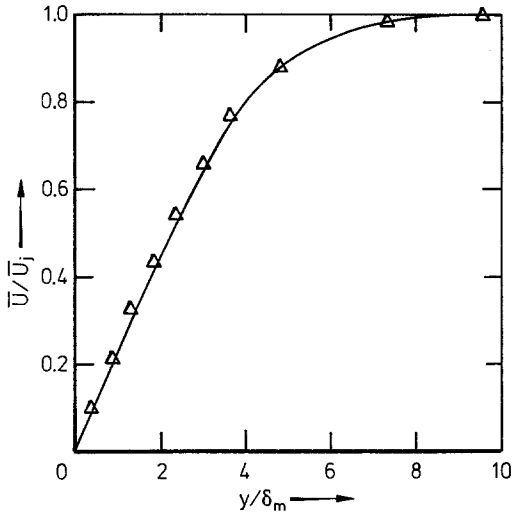

Fig. 2. Initial velocity profile for A. Present: Δ; —— Blasius distribution

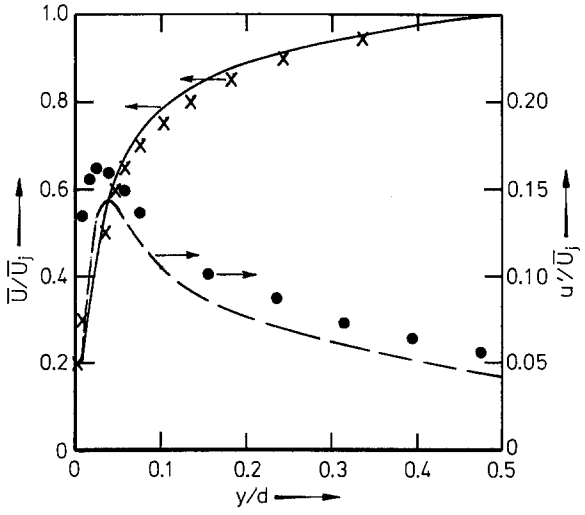

Fig. 3. Initial mean velocity and rms longitudinal velocity for B. $\bar{U}/\bar{U}_j$: × present, —— Shah et al. (1984); $u'/\bar{U}_j$: ● present, -- Shah et al. (1984)

symmetrical about the centreline and a very good approximation to the laminar top-hat distribution. The momentum thickness δ_m of the boundary layer was 0.018 d. The fluctuating intensities of longitudinal velocity $u'/\bar{U}_j$ and temperature $\theta'/\bar{T}_j$ were equal to about 0.2% at the jet centreline.

The mean velocity and turbulent intensities at the exit for B, shown in Fig. 3, compare favourably with the corresponding results (Shah et al. 1984) in a fully developed duct flow at $R_d = 6600$.

3 Flow visualisation

The set up for schlieren photography was similar to that described by Liepmann and Roshko (1957). Two concave mirrors of diameter 10.2 cm and focal length 93.6 cm were used to direct light from a source slit across the test section, a region close to the nozzle exit where x/d ranges from 0 to about 7, onto a knife edge. From the knife edge the image of the test section was directly focused onto a photographic plate or the glass screen of a 10.2 cm × 12.7 cm Linhof Technika camera. The light source was a 1538-A General Radio Co. Strobatac. It was possible to single pulse the Strobatac and hence "freeze" images of instantaneous temperature gradients within the test section onto the camera. The long axis of the light source slit and knife edge could be aligned either parallel or perpendicular to the x axis. The schlieren photographs highlight temperature gradients normal to the knife edge.

Examples of schlieren photographs for A and B are shown in Figs. 4 and 5 respectively. In Fig. 4a the knife edge is parallel to the x direction, while in Fig. 4b and Fig. 5 the knife edge is perpendicular to the x direction. Each photograph shows two rods which give an approximate indication of the distance from the nozzle exit (the rod locations are accurate to $\pm 0.3\, x/d$). The mixing layers show up as darker and lighter regions on the edges of the jet due to the refraction of the light caused by the temperature gradient and the interference of the knife edge.

The structures seen in Fig. 4 are typical of those observed in a large number of photographs. Figure 4 clearly indicates mixing layer structures that are symmetric with respect to the jet centreline. Structures first appear at about $x/d = 1$ and by about $x/d \simeq 4-5$ the two mixing layers are interacting and any organised pattern becomes blurred. It should be recalled however that due to the spanwise integration inherent in the schlieren technique, the three-dimensionality of the structures, resulting from the strong interaction across the jet centreline, would

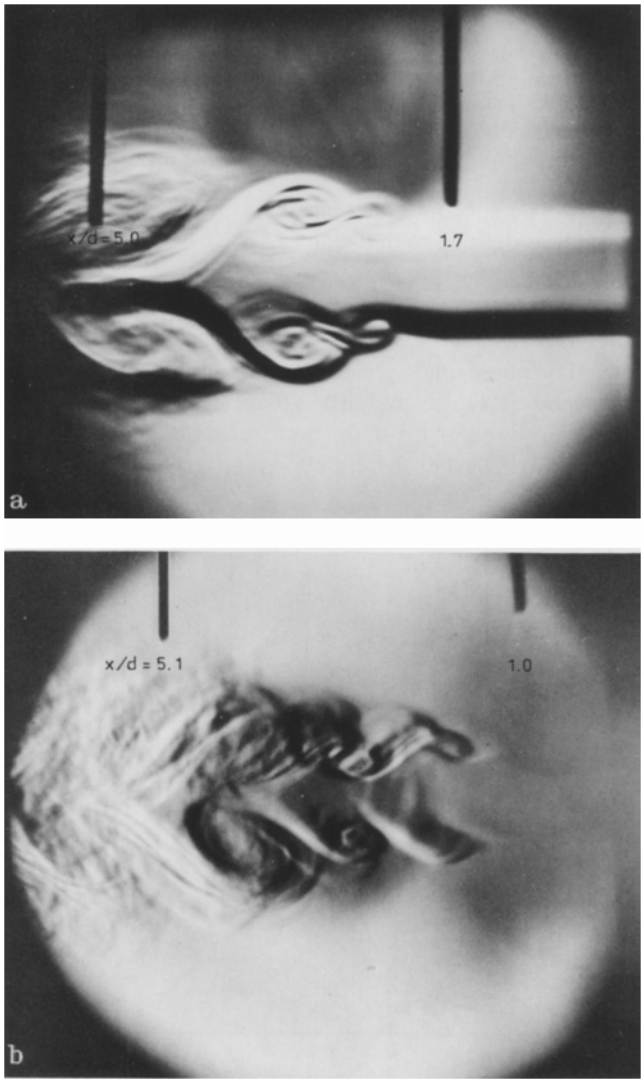

Fig. 4a and b. Schlieren photographs for A. Flow is right to left; **a** knife edge parallel to x; **b** knife edge perpendicular to x

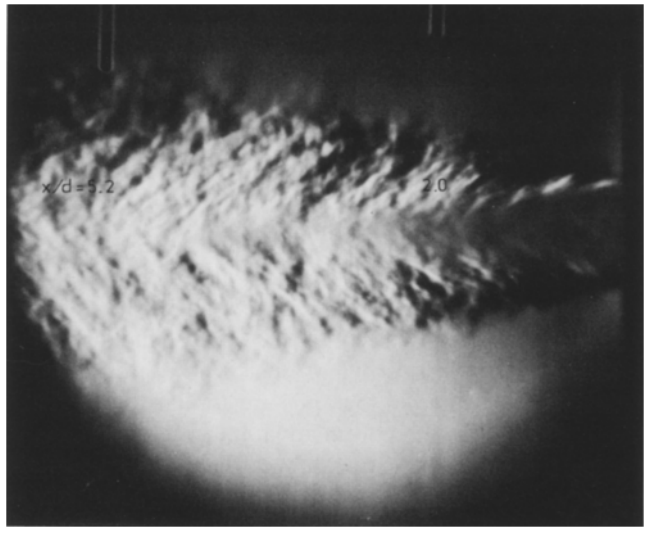

Fig. 5. Schlieren photographs for B. Flow is right to left. Knife edge perpendicular to x

preclude their identification in Fig. 4. Using the same argument, the structures must be reasonably two-dimensional in the region $x/d \lesssim 4$. For x/d greater than about 5, the pattern is somewhat similar to that corresponding to the turbulent profile initial conditions seen in Fig. 5.

It seems pertinent to briefly compare the information in Fig. 4 with that available from flow visualization experiments, reported in the literature, for the near field of a plane jet with initially thin laminar boundary layers. Hussain (1983) describes the instability of the laminar shear layers, roll up, pairing and breakdown of structures in the two shear layers. Most, if not all, of these features, can be observed in the present photographs (Figs. 4a, b). Hussain also mentions the phenomenon of pairing of structures across the centreline, due apparently to the entanglement of one vortical structure by the induced field of another on the opposite side of the plane of symmetry. This feature was not observed in the present series of photographs. The schlieren photographs of Hill et al. (1976) or Hill (1976)[2] indicate that, for conditions similar to A, a symmetric mode is most likely but it is difficult to see one of the mixing layers in the photographs. The violent breakdown of the mixing layers seems to occur near $x/d = 4$. The hydrogen bubble photographs of Rockwell and Niccolls (1972) [their Fig. 6 for which $R_d = 5220$] exhibit features that are closely similar to Fig. 4b. In particular, the potential core flow appears to be highly strained by the opposite mixing layer structures while the spatial extent of the core fluctuates with time. Rockwell and Niccolls also detected an oscillation between symmetric and asymmetric modes but this feature was not apparent in the present photographs. For Krothapalli et al.'s (1981) measurements in the near field of a plane jet, the initial boundary layers were laminar but it is difficult to discern any evidence of symmetry in their published photograph. Several features in the photographs of Fig. 4 can be observed in the smoke photographs, obtained with a sheet of light illuminating a thin central plane of the flow, published for the near field of a circular jet (Crow & Champagne 1971; and more recently Balint et al. 1983). There are however important differences, the symmetric disposition of the structures in the circular jet being associated with toroidal vortex rings.

A typical schlieren photograph (Fig. 5) for B, with the knife edge perpendicular to x, does not indicate evidence of organised structures in the mixing layers, but, as noted earlier, the schlieren technique will not reveal the existence of three-dimensional structures such as presumably occur in a fully developed turbulent duct flow. With the knife edge horizontal, the photographs are similar to Fig. 5 and are not presented. There is an apparent alignment in Fig. 5 of hair-like filaments within the individual mixing layers ($x/d \lesssim 4$) and in the interaction region ($x/d > 4$), of about 140° to the positive x direction. This direction seems to correspond to that of the principal strain rate which is given by $\frac{1}{2}\tan^{-1}(\frac{1}{2}\partial\bar{U}/\partial y)/(\partial\bar{U}/\partial x)$, e.g. Corrsin 1957. This angle does not vary significantly between different flows, its magnitude being about 45° or 135°, as is the case for the present flows. For A, the inclination to the horizontal axis of the braids (Fig. 4b) connecting adjacent structures is about 135°.

4 Results obtained with hot and cold wires

Two cold wires were located at $x/d = 4$ on opposite sides ($y = 0$ and $y = d$, Fig. 1) of the jet centreline to enable measurements of spectral coherences between temperature fluctuations in opposite mixing layers. The location $x/d = 4$ was chosen as it occurs upstream of the region of strong interaction and breakdown of the symmetric structures, at least for A. One-dimensional spectra and cross spectra were first obtained by Fourier transforming the time series corresponding to the temperature fluctuations. The spectral density φ_θ of temperature is defined so that $\int_0^\infty \varphi_\theta(f^*)\,df^* = 1$, where $f^* = 2\pi f x/\bar{U}_j$ and f is the frequency. The spectral coherence Coh between fluctuations θ_1 and θ_2 is defined so that $\mathrm{Coh}(f^*) = (\mathrm{Co}^2 + Q^2)/(\varphi_{\theta_1}\varphi_{\theta_2})$, where Co is the co-spectrum defined such that $\int_0^\infty \mathrm{Co}(f^*)\,df^* = \overline{\theta_1\theta_2}/\theta_1'\theta_2'$, and Q is the quadrature spectrum. The phase angle γ is $\tan^{-1}(Q/\mathrm{Co})$.

Spectra of θ measured at $y = 0$ are in quite good agreement with those at $y = d$, for both A and B and are shown in Fig. 6. However, spectra for A differ markedly from

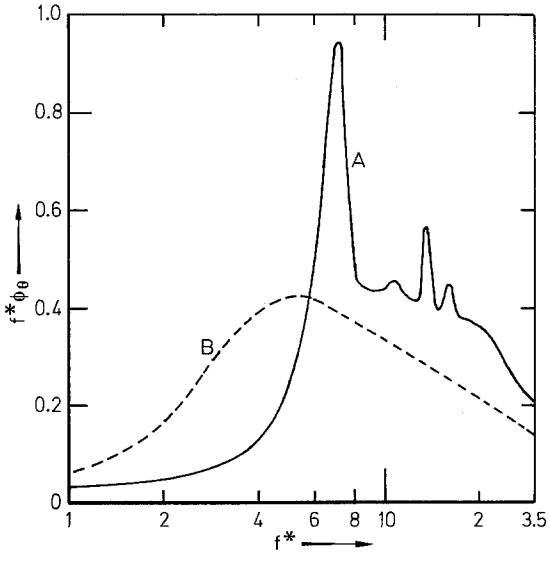

Fig. 6. Spectral density, multiplied by the frequency, at $x/d = 4$ and $y = 0$ or $y = d$. —— A; – – B

2 The Schlieren photographs appearing in Hill (1976) are of better quality and cover a wider range of flow conditions than those in Hill et al. (1976)

those of B. For A, a dominant peak occurs in $f^* \varphi_\theta$ at $f^* = 7$ and secondary peaks at $f^* = 10.5$, 13.5 and 16. For B, the distribution of $f^* \varphi_\theta$ is relatively smooth and exhibits a mild peak at $f^* = 5$. The absence of a dominant peak for B reflects the expectation that, if there is an organised motion, the organisation is only weak. Although it may be argued that long-time averaged coherence measurements are not well suited for revealing the existence of such a motion, such measurements have correctly identified the large scale motion in the nearly self-preserving region of the plane jet (Cervantes & Goldschmidt 1981; Antonia et al. 1983b).

The distributions for the spectral coherence and phase (Fig. 7) differ significantly between A and B. For A, Coh is greater than 0.1 in the frequency range $4 < f^* < 18$ and

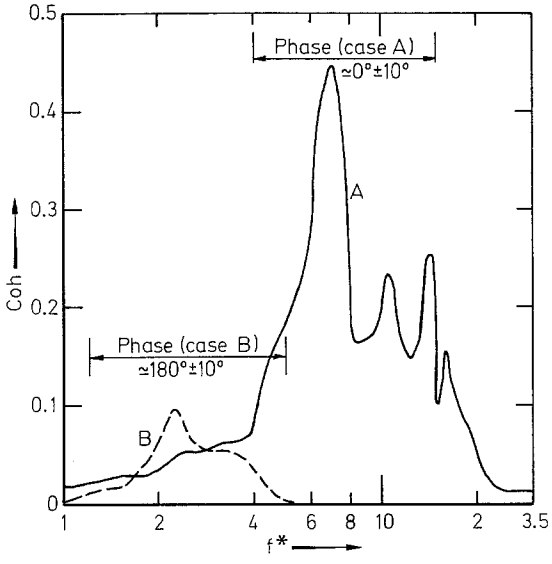

Fig. 7. Spectral coherence at $x/d = 4$ between temperature fluctuations at $y = 0$ and $y = d$. — A; -- B

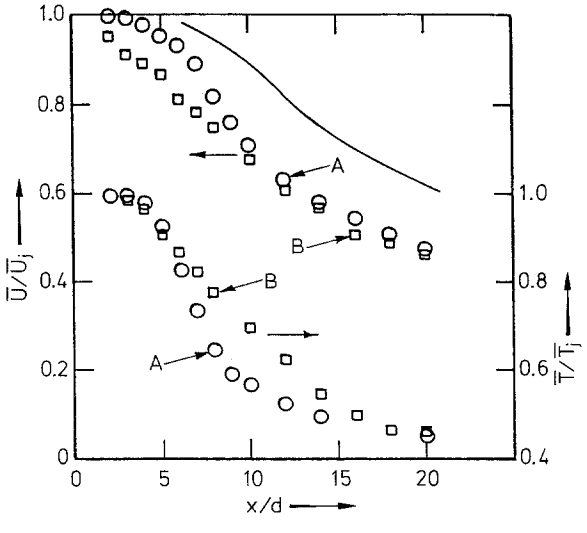

Fig. 8. Centreline distributions of mean velocity and temperature. — $\bar{U}/\bar{U}_j$ (Weir et al. 1981)

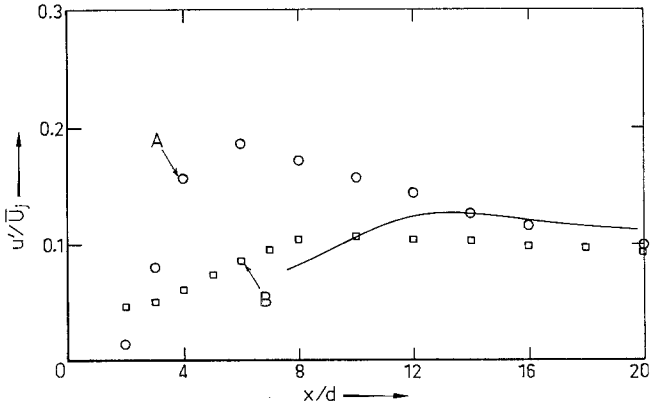

Fig. 9. Centreline distributions of rms velocity. — $u'/\bar{U}_j$ (Weir et al. 1981)

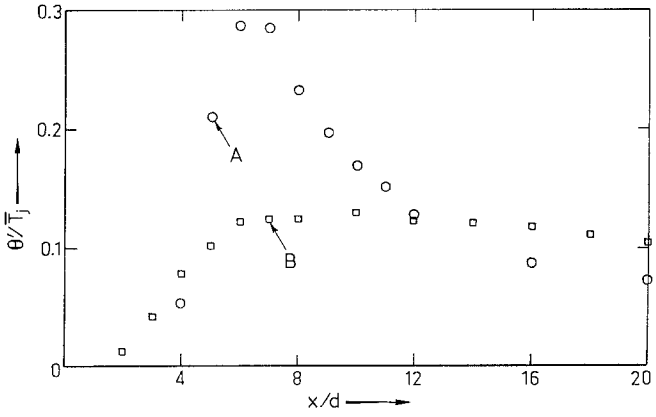

Fig. 10. Centreline distributions of rms temperature. ● A; □ B

exhibits a dominant peak at the same f^* values as in Fig. 6. In the frequency range $4 < f^* < 18$, γ is about 0° (± 10°), confirming the symmetry of the mixing layer structures about the centreline. For B, the magnitude of Coh is, as expected, much smaller than for A. In particular the maximum value of Coh occurs at $f^* = 2.2$ and in the range $1.2 < f^* < 5$, γ is about 180° (± 10°), indicative of asymmetry. Note that the magnitude of the coherence for B, corresponding to the peak in $f^* \varphi_\theta$ (Fig. 6), is negligible.

Centreline distributions of mean velocity, mean temperature, $u'/\bar{U}_j$ and $\theta'/\bar{T}_j$, are shown in Figs. 8–10 up to $x/d = 20$, which corresponds approximately to the beginning of the self-preserving far field region. Estimates of the random uncertainty for measurements of $\bar{U}$, $\bar{T}$, u', θ' were ± 1.5, ± 2, ± 5 and ± 5% respectively. These estimates were inferred from inaccuracies in the calibration data and scatter observed by repeating measurements. Figures 8–10 indicate that there are differences between A and B. Note particularly the relatively large streamwise gradients in $\bar{U}$ and expecially $\bar{T}$ and the large peaks in $u'/\bar{U}_j$ and especially $\theta'/\bar{T}_j$, for case A. The largest gradients and intensities occur at $x/d \simeq 6-7$, apparently resulting from the strong interaction between the sym-

metric coherent structures (Fig. 4). It is interesting to note that the distributions of $\bar{U}/\bar{U}_j$ and $u'/\bar{U}_j$ inferred from the data of Weir et al. (1981) are qualitatively similar to those corresponding to B, although the peak value of $u'/\bar{U}_j$ occurs at a slightly larger value of x/d than for B. Recalling that the nozzle boundary layers were laminar in Weir et al.'s case, the qualitative agreement with B rather than A in Figs. 7 and 8 lends some support to the claim that the interaction is weaker in the case of asymmetric and the three-dimensional structures than for symmetric coherent structures. Figures 8–10 all indicate that changes in mean and rms quantities first occur at larger value of x/d, for A than B. This is clearly associated with the length of the potential core in case A. There is strictly no potential core for case B but Fig. 5 appears to indicate that the regions associated with large temperature gradients merge at $x/d \simeq 3$.

5 Conclusions

Large differences have been found in the interaction region of the jet between configurations A and B. The experimental evidence has shown that, at the nominal end of the potential core, for A, the structures are coherent and symmetrical with respect to the centreline. The ensuing strong interaction between these structures results in strong mixing, as reflected by the large peak values in the rms velocity and rms temperature at $x/d \simeq 6$. For B, neither the schlieren visualisation nor the spectral phase data are inconsistent with the likelihood of asymmetric, three-dimensional structures. The ensuing interaction between structures is weak, as reflected by the relatively small peak values of $u'/\bar{U}_j$ and $\theta'/\bar{T}_j$. The similarity between B and Weir et al.'s (1981) measurements, and the reasonable success of the superposition analysis for Weir et al.'s flow lends indirect support to the contention that the structures are asymmetrically arranged in case B. Browne et al. (1984) have already shown that the superposition analysis does not work for A. From a theoretical viewpoint, cases A and B would require different analytical treatments if the interaction region were to be correctly calculated.

It is likely that other flow geometries, such as for example initially turbulent boundary layers separated by a non-turbulent core, could lead to results similar to those obtained with B. With respect to A, the way in which symmetric structures interact and how they are eventually replaced by an alternating vortex pattern, as observed in the latter part of the interaction region (Antonia et al. 1983b; Oler & Goldschmidt 1981) are matters that require further investigation. On a practical note, the present evidence suggests that A has advantages over B if the objectives are to promote strong mixing in the interaction region and to achieve self-preservation of the far field in a minimum distance.

Acknowledgements

The assistance of C.S. Teo and L. P. Chua with data reduction is appreciated. The support of the Australian Research Grants Scheme is gratefully acknowledged.

References

Antonia, R. A.; Browne, L. W. B.; Chambers, A. J.; Rajagopalan, S. 1983a: Budget of the temperature variance in a turbulent plane jet. Int. J. Heat Mass Transf. 26, 41–48

Antonia, R. A.; Browne, L. W. B.; Rajagopalan, S.; Chambers, A. J. 1983b: On the organised motion of a turbulent plane jet. J. Fluid Mech. 134, 49–66

Balint, J.-L.; Molines, J.-M.; Ayrault, M.; Schon, J.-P.; Mathieu, J. 1983: Etude du champ de concentration d'un jet rond par une méthode de visualisation quantitative. C. R. Acad. Sc. Paris, 296, 1011–1014

Browne, L. W. B.; Antonia, R. A.; Chambers, A. J. 1984: The interaction region of a turbulent plane jet. J. Fluid Mech. 149, 355–373

Cervantes de Gortari, J.; Goldschmidt, V. W. 1981: The apparent flapping motion of a turbulent plane jet – Further experimental results. J. Fluids Eng. 103, 119–126

Comte-Bellot, G. 1963: Contribution à l'étude de la turbulence de conduite. P. S. T. Ministère de l'Air, No. 419. (English translation by P. Bradshaw, 1969 – Report ARC 31 609)

Corrsin, S. 1957: Some current problems in turbulent shear flows. Proc. 1st Nav. Hydr. Symp., Nat. Acad. Sci./Nat. Res. Counc., Washington, D.C., Pub. No. 515

Crow, S. C.; Champagne, F. H. 1971: Orderly structure in jet turbulence. J. Fluid Mech. 48, 547–591

Dean, R. B.; Bradshaw, P. 1976: Measurements of interacting turbulent shear layers in a duct. J. Fluid Mech. 78, 641–676

Hill, W. G. 1976: Flow visualization investigation of the effects of initial boundary layer on jet mixing. Grumman Res. Dep. Memorandum RM-612, Bethpage, New York

Hill, W. G.; Jenkins, R. C.; Gilbert, B. L. 1976: Effects of the initial boundary layer state on turbulent jet mixing. AIAA J. 14, 1513–1514

Hussain, A. K. M. F. 1983: Coherent structures – Reality and myth. Phys. Fluids 26, 2816–2850

Krothapalli, A.; Baganoff, D.; Karamcheti, K. 1981: On the mixing of a rectangular jet. J. Fluid Mech. 107, 201–220

Liepmann, H. W.; Roshko, A. 1957: *Elements of gasdynamics*, p. 157. New York: Wiley

Oler, J. W.; Goldschmidt, V. W. 1981: Coherent structures in the similarity region of two-dimensional turbulent jets. Proc. Third Symposium on Turbulent Shear Flows, Davis, 11.1

Oseberg, O. K.; Kline, S. J. 1971: The near field of a plane jet with several initial conditions. Rep. MD-28, Dep. Mech. Eng., Stanford University

Rockwell, D. O.; Niccolls, W. O. 1972: Breakdown of planar jet. J. Basic Eng. 94, 720–730

Shah, D. A.; Antonia, R. A.; Chambers, A. J. 1984: Scaling of the "Bursting" frequency in a turbulent duct flow. TNFM12, Dept. Mech. Eng., University of Newcastle

Weir, A. D.; Bradshaw, P. 1975: Resonance and other oscillations in the initial region of a plane turbulent jet. Rep. 75-07, Dep. Aeronautics, Imperial College

Weir, A. D.; Wood, D. H.; Bradshaw, P. 1981: Interacting turbulent shear layers in a plane jet. J. Fluid Mech. 107, 237–260

Received November 7, 1984